

## Supplementary information

### Low lattice thermal conductivity and promising thermoelectric figure of merit of Zintl type $\text{TlInTe}_2$

Guangqian Ding<sup>a</sup>, Junjie He<sup>a</sup>, Zhenxiang Cheng<sup>\*b</sup>, Xiaotian Wang<sup>\*c</sup> and Shuo Li<sup>d</sup>

<sup>a</sup>Institute for Quantum Information and Spintronics (IQIS), School of Science, Chongqing University of Posts and Telecommunications, Chongqing, 400065, People's Republic of China.

<sup>b</sup>Institute for Superconducting & Electronic Materials (ISEM), University of Wollongong, Wollongong, 2500, Australia.

<sup>c</sup>School of Physical Science and Technology, Southwest University, Chongqing, 400715, People's Republic of China.

<sup>d</sup>Department of Physical and Macromolecular Chemistry, Faculty of Science, Charles, University in Prague, 128 43 Prague 2, Czech Republic.

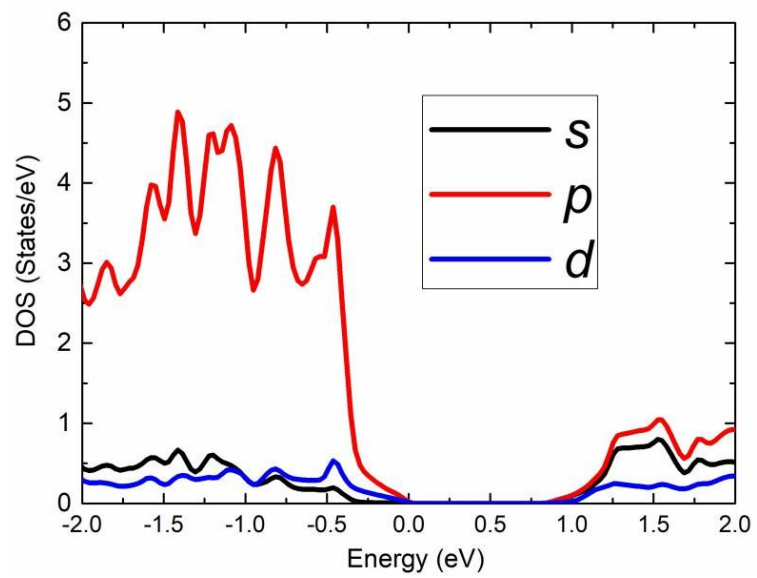


**Fig. S1.** Contribution of different atomic state to the density of states in TlInTe<sub>2</sub>.

**Table S1.** Calculated elastic constant  $C$ , carrier effective mass  $m^*$ , deformation potential (DP) constant  $E$ , and relaxation time  $\tau$  of TlInTe<sub>2</sub> at room temperature.

Carriers	$C$ (eV/Å <sup>3</sup> )	$m^*$ ( $m_e$ )	$E$ (eV)	$\tau$ (10 <sup>-14</sup> s)
Hole	3.45	0.2	-34.05	18
Electron	3.45	0.47	-26.78	9.8

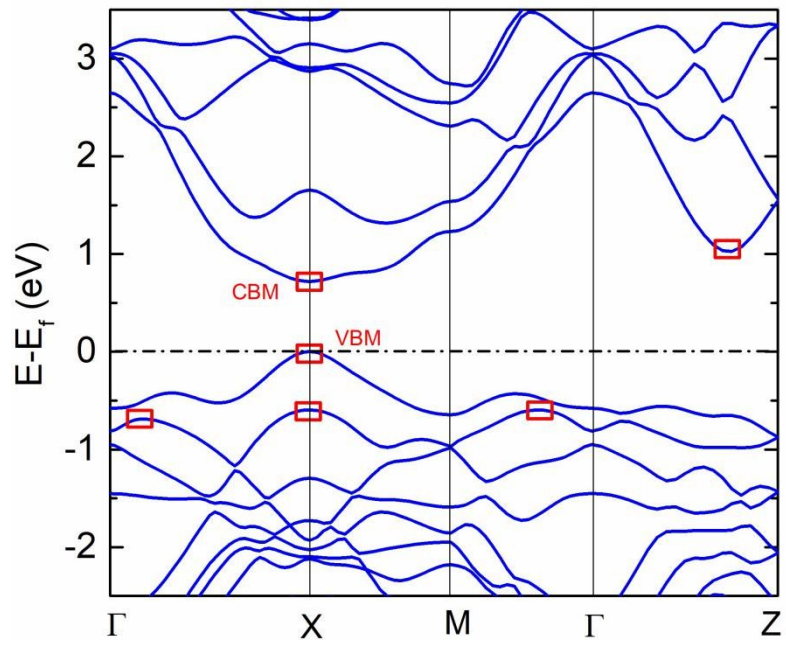


**Fig. S2.** Calculated band structure of TlGaTe<sub>2</sub>.

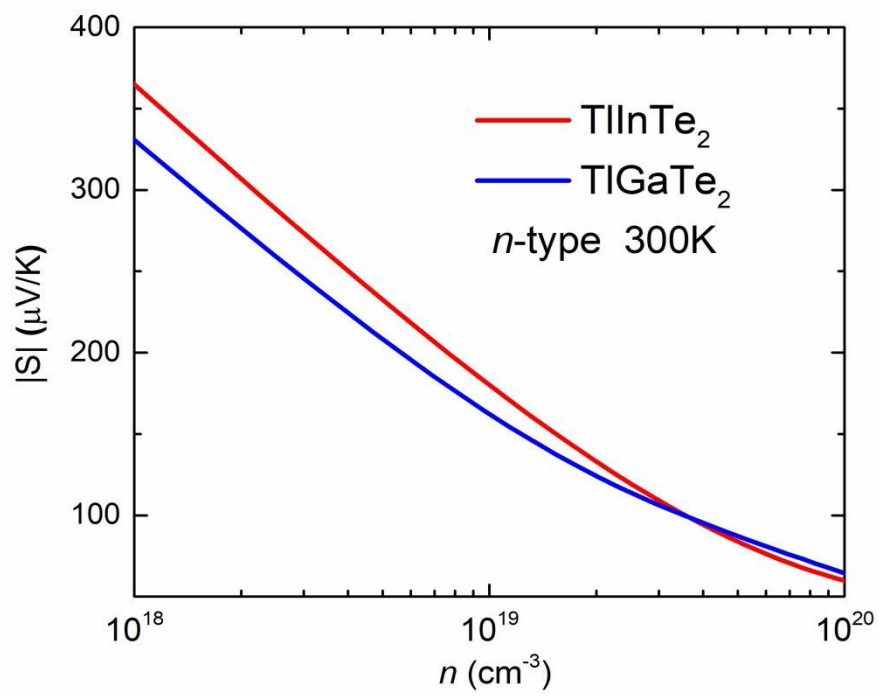


**Fig. S3.** Comparison of  $n$ -type Seebeck coefficient between  $\text{TlInTe}_2$  and  $\text{TlGaTe}_2$  at

300K.